

## Binder Rheology Based Dynamic Modulus and Phase Angle Predictive Models for Asphalt Concrete

A. S. M. Asifur Rahman<sup>1</sup>; Umme A. Mannan<sup>2</sup>; and Rafiqul A. Tarefder<sup>3</sup>

<sup>1</sup>Ph.D. Candidate, Civil Engineering, MSC01 1070, 1 University of New Mexico, Albuquerque, NM 87131. E-mail: [arahman@unm.edu](mailto:arahman@unm.edu)

<sup>2</sup>Ph.D. Candidate, Civil Engineering, MSC01 1070, 1 University of New Mexico, Albuquerque, NM 87131. E-mail: [uam@unm.edu](mailto:uam@unm.edu)

<sup>3</sup>Professor, Civil Engineering, MSC01 1070, 1 University of New Mexico, Albuquerque, NM 87131. E-mail: [tarefder@unm.edu](mailto:tarefder@unm.edu)

### Abstract

This study proposes new regression-based predictive models to estimate dynamic modulus and phase angle of asphalt concrete from the dynamic shear modulus and phase angle of the asphalt binder used in the asphalt mixture. Other parameters related to the aggregate gradation and mixture volumetric are also incorporated in these models. A total of 10 asphalt concrete mixes with 4 asphalt binders having different performance grades and sources were used in this study. The loose asphalt-aggregate mixtures were compacted and cored to cylindrical specimens. Three cylindrical specimens from each of the asphalt-aggregate mixtures were prepared and tested in the laboratory for dynamic modulus and phase angle at different test temperatures and loading frequencies. For all the test specimens, dynamic modulus and phase angle mastercurves at 70 °F reference temperature were generated by applying time-temperature superposition principle. The collected binders were tested for dynamic shear modulus and binder phase angle using dynamic shear rheometer. Also for the binder, the dynamic shear modulus and phase angle mastercurves were generated by applying time-temperature superposition principle. Non-linear optimization process was used to evaluate the model parameters. Statistical analysis showed that a fairly accurate estimation of dynamic modulus as well as phase angle of asphalt concrete as a function of temperature and loading frequency can be found by using these new predictive models.

### INTRODUCTION

The complex modulus ( $E^*$ ) is a complex number that relates applied stress to the strain for a linear viscoelastic material subjected to sinusoidal loading. The two material functions that can be determined from  $E^*$ -test are the dynamic modulus and the phase angle. The absolute value of  $E^*$  is referred to as dynamic modulus ( $|E^*|$ ), whereas, the time lag between the applied stress and the strain response is referred as the angle ( $\phi$ ). In case of asphalt concrete (AC), determining broadband  $|E^*|$  and  $\phi$ -functions involve application of sinusoidal load at various frequencies and temperatures and the measurement of resulting strain and the time-lag between the applied stress and the resulting strain. This ultimately enable us to apply time-temperature superposition principle to obtain the  $|E^*|$  and  $\phi$ -functions.

The  $|E^*|$  of AC depends on many factors. Several empirical models are available in the literature addressing these factors to determine  $|E^*|$  of AC, of which, the most commonly used are the viscosity ( $\eta$ ) based Witczak model, the binder shear modulus ( $|G_b^*|$ ) based Witczak model, and the Hirsch model (Weldegiorgis 2014). The  $\eta$ -based Witczak model is the primary  $|E^*|$  predictive model in the recent mechanistic-empirical pavement design software AASHTOWare-ME (Andrei et al. 1999). The performance of the  $\eta$ -based Witczak model was evaluated by a number of researchers. Clyne et al. (2003), Christensen et al. (2003), Tran and

Hall (2005), Schwartz (2005), and Mohammad et al. (2005) reported that the  $\eta$ -based Witczak model produces less value of  $|E^*|$ . Lee et al. (2007) found that the  $|E^*|$  predicted by the  $\eta$ -based Witczak model gives lower  $|E^*|$ -values at higher temperature and higher  $|E^*|$ -values at lower temperature. Hossain and Zaman (2013) concluded that the  $\eta$ -based Witczak model significantly underestimate  $|E^*|$  with the  $|G_b^*|$  test data, however, the model overestimates  $|E^*|$  when rotational viscosity (RV) test data is used. Birgisson et al. (2005) found an over prediction of  $|E^*|$  by the  $\eta$ -based Witczak model.

The  $|G_b^*|$ -based Witczak model (Bari and Witczak 2006) was developed using the Bari (2005) database of 7400 measured  $|E^*|$ -values obtained from 346 different AC mixtures. The data used in earlier version of the model were included in this expanded database. The viscosity of the asphalt binder was determined from the ASTM viscosity temperature relationship (ASTM 1998). However, to convert conventional viscosity-temperature susceptibility parameters,  $A$  and  $VTS$  to  $|G_b^*|$  and binder phase angle ( $\delta_b$ ), empirical models were also provided due to absence of test data (Ceylan 2009). Also, issues have been raised regarding the use of inconsistent treatment of loading frequency in case of AC mix and asphalt binder (Christiansen 2006). Singh et al. (2011) reported that the accuracy of the  $|G_b^*|$ -based Witczak model is poor. El-Badawy et al. (2012) reported that  $|G_b^*|$ -based model produced less accurate and higher biased estimates of  $|E^*|$  than the  $\eta$ -based Witczak model.

Christensen et al. (2003) found the most effective version of Hirsch model in which  $|E^*|$  is directly estimated from binder  $|G_b^*|$ , voids in mineral aggregate (VMA), and voids filled with asphalt binder (VFA). Singh et al. (2011) also investigated this model and found that the model exhibits significant error. Bari and Witczak (2006), Obulareddy (2006), King et al. (2005), and Ceylan et al. (2008) reported that the Hirsch model underpredicts  $|E^*|$ . However, the fundamental weakness of this model is the strong dependence on volumetric parameters (Soleymani et al. 2004).

## OBJECTIVE

The objective of this study is to develop an alternative, more accurate  $|E^*|$  and  $\phi$  predictive models for the AC mixtures typically used in New Mexico. The model should be capable of reflecting changes in  $|E^*|$  as a function of aggregate gradation, volumetric, binder property, temperature and loading frequency. Nonlinear regression was used for the development of the models. To incorporate the aggregate gradation, two universally known gradation parameters, the uniformity coefficient ( $C_u$ ) and the fineness modulus ( $F_m$ ) are introduced in the models instead of using directly the percentage of material retained or passing on a particular sieve which is very common in most of the  $|E^*|$  models currently in practice. It should be noted that, the  $F_m$  which is an empirical figure, introduced in this study is slightly different than the conventional  $F_m$ . In determining the conventional  $F_m$ , the sieve-size increases in the ratio of 2:1. However, in current study, all the sieves used for Superpave gradation analysis are considered for determining the  $F_m$  of the aggregate. The deviation from the standard definition of  $F_m$  is introduced to incorporate all the sieves used in the Superpave gradation analysis and also to attain considerable ease while determining  $F_m$ . The alternative definition of  $F_m$  is also consistent with the fundamental concept regarding  $F_m$  that a smaller value indicating relatively finer aggregate type.

## MATERIALS AND PREPARATION OF TEST SPECIMENS

**Materials.** A total of ten loose AC mixtures (referred as Mix-1 through Mix-10) with four asphalt binders of different PG grades were collected from the paving sites in New Mexico. On

the other hand, liquid asphalt binders used in the AC mixtures were collected from the asphalt mixing plants. A summary of the collected AC mixtures and binders are presented in Table 1.

**Preparation of Test Specimens.** A Superpave® gyratory compactor was used to compact loose AC mixtures according to AASHTO T 312 specification. Cylindrical AC cores of diameter 150 mm and of height 170 mm were compacted. The range of air void content is set at  $5.5 \pm 0.5\%$  for the finished specimens. The compacted samples were then core-drilled and sawed to finished specimens of diameter 100 mm and of height 150 mm. The theoretical maximum specific gravity ( $G_{mm}$ ) was determined by AASHTO T 209 specification. The bulk specific gravity ( $G_{mb}$ ) was determined according to AASHTO T 166 standard protocol. For each AC mixture, 3 cylindrical specimens were prepared. AASHTO T 240 standard was used to conduct RTFO aging of the collected virgin binders.

**Table 1. Summary of Collected Asphalt Concrete Mixtures and Asphalt Binders**

Mix ID	Superpave Gradation	Nominal Maximum Aggregate Size (NMAS), mm	Asphalt Binder Performance Grade (PG)	Type of Aggregate Material
Mix 1	SP IV	12.5	PG 64-22	Alluvial Limestone
Mix 2	SP III	19.0	PG 64-28	Sand & Gravel
Mix 3	SP III	19.0	PG 76-28	Dacite
Mix 4	SP III	19.0	PG 76-28	Basalt
Mix 5	SP III	19.0	PG 76-22	Sand & Gravel
Mix 6	SP III	19.0	PG 64-28	Basalt
Mix 7	SP III	19.0	PG 64-22	Limestone (Source 1)
Mix 8	SP III	19.0	PG 64-22	Limestone (Source 2)
Mix 9	SP III	19.0	PG 64-22	River Deposits
Mix 10	SP III	19.0	PG 64-28	River Deposits

## LABORATORY TESTS

**Complex Modulus Test.** The  $|E^*|$  with  $\phi$  testing was conducted according to AASHTO T 342 test protocol. In short, all the AC specimens were tested for  $|E^*|$  at five different test-temperatures of 14, 40, 70, 100, and 130 °F and six loading frequencies of 25, 10, 5, 1, 0.5, and 0.1 Hz.

**Frequency Sweep Complex Shear Modulus Test.** The AASHTO T 315 test standard was employed as a guideline for conducting dynamic shear modulus,  $|G_b^*|$  and phase angle ( $\delta_b$ ) testing on the binder samples using a dynamic shear rheometer (DSR). The  $|G_b^*|$  with  $\delta_b$  tests were conducted at test-temperatures of 130, 115, 100, 85, 70, 55, and 40 °F, and at 11 frequencies ranging from 1.0 to 100 rad/sec. Binder specimens with 8 mm in diameter and 2 mm in height were used to conduct  $|G_b^*|$  tests. The tests are conducted in a strain controlled mechanism and the applied strain level was 1.0% as suggested by Weldegiorgis et al. (2013).

## THE MASTERCURVES

**Dynamic Modulus and Dynamic Shear Modulus.** The time-temperature superposition principal (TTSP) was applied to develop the average  $|E^*|$ - mastercurves for the AC mixtures and the  $|G_b^*|$ -mastercurves for the binders at 70 °F reference temperature. As both the  $|E^*|$  and  $|G_b^*|$  functions follow sigmoid shape, the following sigmoid expression was used to fit these functions

$$\log |F(\omega)| = \delta_{MC} + \frac{\alpha}{1 + e^{\beta + \gamma \log(\omega)}} \quad (1)$$

In Eq.(1),  $F(\omega)$  is the material function, i.e.  $|E^*(\omega)|$  for AC mixtures, and  $|G_b^*(\omega)|$  for the binders. Note that, both of these functions are kept in angular frequency space, designated by  $\omega$ . The relationship between  $\omega$  in rad/sec and ordinary frequency ( $f$ ) in Hz is defined as,  $\omega = 2\pi f$ . The other parameters in Eq.(1), such as,  $\omega_r$  is the reduced angular frequency of loading, and  $\alpha, \beta, \gamma, \delta_{MC}$  are the fitting parameters. Figure 1(a) shows the tested  $|E^*|$  versus loading frequency (in Hz) plot at different test temperatures for one of the cylindrical specimens of AC Mix-1. The figure also shows TTSP applied horizontally shifted  $|E^*|$  data along the ordinary frequency space to construct  $|E^*|$ -mastercurve. After a smooth representation of  $|E^*|$  data was found by applying TTSP, the  $|E^*|$  mastercurves (discrete data points) were fitted by Eq.(1). Once the  $|E^*|$ -mastercurve was fitted, the relationship  $\omega = 2\pi f$  was used to transform ordinary frequency space into angular frequency space. Similarly, Figure 1(b) shows  $|G_b^*(\omega)|$  versus loading frequency (in rad/s) plots at different test temperatures for the PG 64-22 binder. Note that, the  $|G_b^*(\omega)|$  data was already in angular frequency space, and therefore, no transformation was necessary. The figure also shows TTSP applied horizontally shifted  $|G_b^*(\omega)|$  data. Finally, the generated mastercurve was fitted by Equation 1.

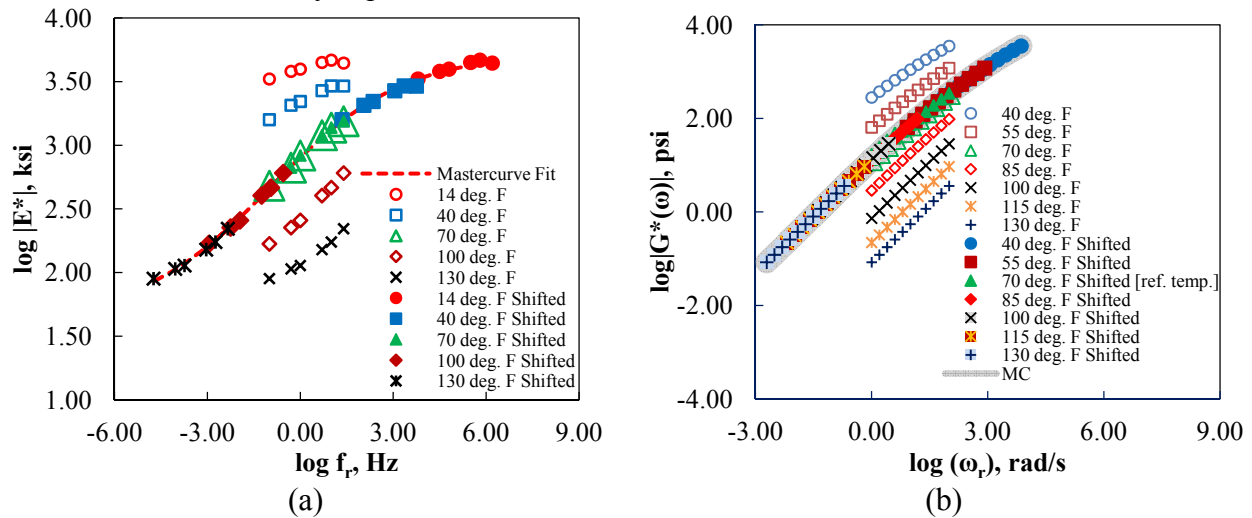


Figure 1. (a)  $|E^*|$ -mastercurve for the AC specimen, and (b)  $|G_b^*(\omega)|$ -mastercurve for the binder at 70 °F reference temperature.

**Phase Angles of Asphalt Concrete and Asphalt Binder.** The phase angle mastercurves at 70 °F reference temperature for the AC specimens as well as for the binders were generated by using the same frequency-temperature shift factors found while developing  $|E^*(\omega)|$  or,  $|G_b^*(\omega)|$ -mastercurves. The  $\phi$ -mastercurves of the AC specimens and the  $\delta_b$ -mastercurves of the asphalt binders were then fitted by the expression suggested by Rahman et al. (2016) for AC mixtures, and found to be equally applicable for  $\delta_b$ -functions of asphalt binders, and can be give as -

$$\theta(\omega) = \xi_1 + \xi_2 \log(\omega_r) - \xi_3 \frac{\pi}{2} \alpha \gamma \frac{e^{\beta + \gamma \log(\omega_r)}}{\left(1 + e^{\beta + \gamma \log(\omega_r)}\right)^2} \quad (2)$$

Here,  $\theta(\omega)$  is the phase angle function, i.e.  $\phi(\omega)$  for the asphalt specimens, or,  $\delta_b(\omega)$  for the asphalt binders;  $\xi_1, \xi_2$ , and  $\xi_3$  are the regression constants; and  $\alpha, \beta$ , and  $\gamma$  are the corresponding  $|E^*(\omega)|$  or,  $|G_b^*(\omega)|$  fitting parameters. Figure 2(a) shows a typical curve fitting of the  $\phi$ -mastercurve for one of the cylindrical specimens of AC Mix-1, while Figure 2(b) shows a typical curve fitting of  $\delta_b$ -mastercurve of PG 64-22 binder by Eq.(2).

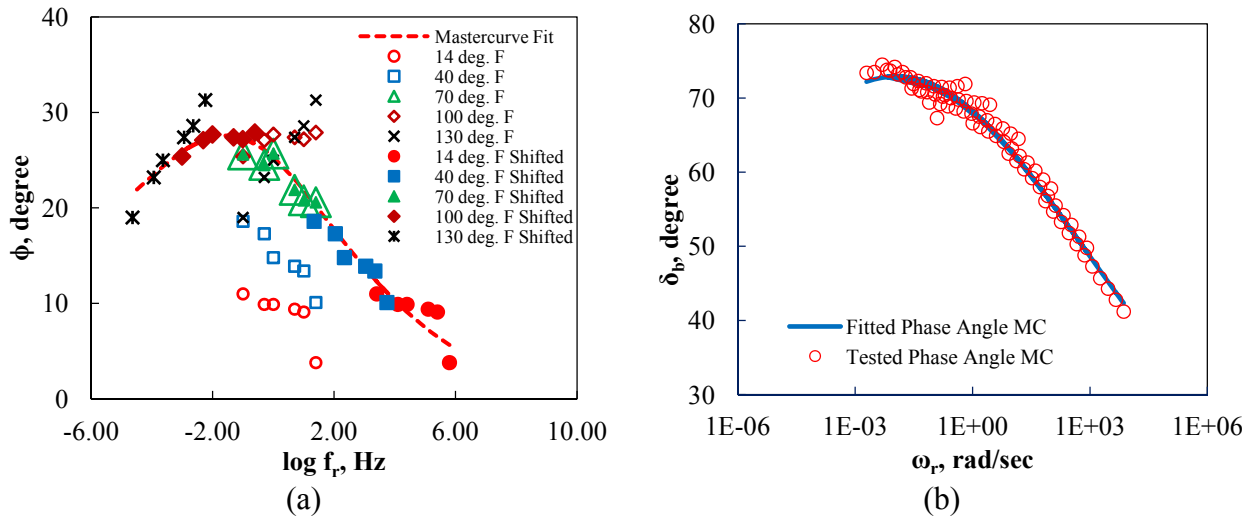


Figure 2. (a)  $\phi$ -mastercurve for the AC specimen, and (b)  $\delta_b$ -mastercurve for the binder at 70 °F reference temperature.

**THE NEW PREDICTIVE MODELS**

For developing new predictive models, nonlinear regression approach was used. In current practice  $|E^*|$  is determined in ordinary frequency space, while  $|G_b^*|$  is determined in angular frequency space. Therefore, to study the effect of binder properties in the proposed model, it was necessary to convert the ordinary frequency space to angular frequency space in case of  $|E^*|$  functions of the AC mixtures. The variables affecting  $|E^*(\omega)|$  of AC mixtures considered are:  $F_m$ , and  $C_u$  for the aggregate blend used in the AC mixtures; effective percent volumes of the asphalt binders ( $V_{beff}$ ), percent air voids ( $V_a$ ) in the cylindrical AC specimens,  $|G_b^*(\omega)|$  and the associated  $\delta_b$  of the binders at a given loading frequency. The definitions of  $F_m$ , and  $C_u$  can be given as:

$$F_m = \frac{\sum_{i=1}^n CPR_i}{100}, \text{ and } C_u = \frac{D_{60}}{D_{10}}. \tag{3}$$

Here,  $CPR_i$  is the cumulative percentage of aggregate retained at  $i^{th}$  sieve used in Superpave gradation analysis,  $D_{60}$  is the sieve size corresponding to 60% material passing,  $D_{10}$  is the sieve size corresponding to 10% material passing, and  $n$  is the number of sieves used in the sieve analysis. A total of 13 standard sieves were used for sieve analyses of the aggregate blends. The designation and the opening sizes of the sieves are presented in Table 2.

**Table 2. Standard Sieves and Opening Sizes Used**

Sieve Designation	Sieve Opening (mm)	Sieve Designation	Sieve Opening (mm)
2 inch	50.00	No. 8	2.36
1.5 inch	37.50	No. 16	1.18
1 inch	25.00	No. 30	0.60
3/4 inch	19.00	No. 50	0.30
1/2 inch	12.50	No. 100	0.15
3/8 inch	9.50	No. 200	0.075
No. 4	4.75		

The analysis on aggregate blends are conducted to establish the model parameters. Table 3 summarizes the gradation parameters (i.e.  $F_m$  and  $C_u$ ), and  $V_{beff}$  for 10 aggregate blends used in the AC mixtures. The air void contents ( $V_a$ ) of all 30 cylindrical AC specimens are also listed in Table 3. A two-step modeling approach is adopted while developing the  $|E^*(\omega)|$  as well as the  $\phi(\omega)$  predictive models. In the first step, the first seven AC mixtures and associated binders were used to develop the models, and the modulus and phase angle data of remaining AC mixtures and binders were tested. In the second step, all 10-AC mixtures (30 cylindrical AC specimens) are used to obtain the final form of the predictive models.

**Table 3. Summary of Mix Volumetric and Aggregate Gradation Parameters**

Mix ID	$\sum_{i=1}^n CPR_i$	$D_{60}$	$D_{10}$	$F_m$	$C_u$	$V_{beff}$	$V_a$		
							Specimen 1	Specimen 2	Specimen 3
Mix 1	503.90	4.10	0.11	5.039	37.27	11.26	6.0	6.0	5.2
Mix 2	626.40	8.10	0.22	6.264	36.82	11.54	5.6	5.1	5.7
Mix 3	598.50	6.80	0.23	5.985	29.57	11.23	5.6	5.0	5.0
Mix 4	658.50	10.0	0.30	6.585	33.33	10.52	6.0	5.9	6.0
Mix 5	606.00	6.50	0.22	6.060	29.55	12.04	6.0	6.0	6.0
Mix 6	653.50	10.00	0.22	6.535	31.25	9.39	5.7	5.3	5.3
Mix 7	596.30	6.60	0.18	5.963	36.67	10.88	5.0	5.0	5.8
Mix 8	597.10	6.90	0.15	5.971	46.00	10.54	6.0	5.9	6.0
Mix 9	612.10	6.70	0.18	6.121	37.22	11.05	6.0	5.7	6.0
Mix 10	639.20	10.00	0.22	6.392	45.46	10.12	5.0	5.0	5.0

**Dynamic Modulus Predictive Model.** An effect study showed that the parameters  $\alpha$ ,  $\beta$ , and  $\delta_{MC}$  in Eq.(1) for the AC mixtures are significantly related to the  $F_m$ ,  $C_u$ ,  $V_{beff}$ , and  $V_a$  of the AC sample under concern. However, due to the limitation associated with the length of this paper, the effect study is not presented. After a considerable amount of the trials, the final form of the  $|E^*(\omega)|$  predictive model can be presented by the expression given in Eq.(4). Note that, the  $|E^*(\omega)|$  is kept at angular frequency space so that the angular loading frequency associated with a certain pair of  $|G_b^*|$  and  $\delta_b$  can be readily used in the equation to estimate the  $|E^*(\omega)|$  of the AC mix for that particular angular frequency of loading. In Eq.(4), both the  $|E^*(\omega)|$  and  $|G_b^*(\omega)|$  are in pound per square inch (psi) unit.

$$\log|E^*(\omega)| = 2.98344 - 0.36204(F_m)^{0.5879} - 0.00291(C_u)^{1.6006} + 4.47476\left(\frac{V_{beff}}{V_{beff} + V_a}\right)^{0.78665} + \frac{4.118646(F_m)^{0.161757} + 0.308047(C_u)^{0.608689} - 7.137353\left(\frac{V_{beff}}{V_{beff} + V_a}\right)^{0.588208}}{1 + e^{-1.93502(F_m)^{0.304465} - 0.947132(C_u)^{0.43679} + 8.367143\left(\frac{V_{beff}}{V_{beff} + V_a}\right)^{0.376962} - 0.452361[1.2233 \log|G_b^*(\omega)| - 1.1527 \log \delta_b(\omega)]}} \quad (4)$$

Eq.(9) is analogous to Eq.(3), where –

$$\alpha = 4.118646(F_m)^{0.161757} + 0.308047(C_u)^{0.608689} - 7.137353\left(\frac{V_{beff}}{V_{beff} + V_a}\right)^{0.588208} \quad (5)$$

$$\beta = -1.935020(F_m)^{0.304465} - 0.947132(C_u)^{0.436790} + 8.367143 \left( \frac{V_{beff}}{V_{beff} + V_a} \right)^{0.376962} \quad (6)$$

$$\delta_{MC} = 2.98344 - 0.36204(F_m)^{0.5879} - 0.00291(C_u)^{1.6006} + 4.47476 \left( \frac{V_{beff}}{V_{beff} + V_a} \right)^{0.78665} \quad (7)$$

$$\text{and, } \gamma = -0.452361. \quad (8)$$

**Phase Angle Predictive Model.** The expression given in Eq.(2) was used to develop the  $\phi$  predictive model for asphalt concrete. An effect study showed that the parameters  $\xi_1$ , and  $\xi_3$  are significantly related to the  $F_m$ ,  $C_u$ ,  $V_{beff}$ , and  $V_a$ , while the parameter  $\xi_2$  is significantly related to the  $C_u$ ,  $V_{beff}$ , and  $V_a$  of the AC sample under concern. Again, due to the limitation associated with the length of this paper, the effect study is not presented. The optimized form of the  $\phi$ -predictive model for the AC mix can be given as -

$$\begin{aligned} \phi(\omega) = & -0.75729 - 0.04673 F_m - 0.000051 (C_u)^{2.4065} + 2.00944 \left( \frac{V_{beff}}{V_{beff} + V_a} \right) \\ & + \left[ 0.43604 + 0.03399 (C_u)^{0.53471} - 0.74847 \left( \frac{V_{beff}}{V_{beff} + V_a} \right)^{0.30623} \right] \log(\omega_r) \\ & - \left[ 3.53402 + 0.1047 F_m + 0.00064 (C_u)^{2.04946} - 6.12145 \left( \frac{V_{beff}}{V_{beff} + V_a} \right) \right] \frac{\pi}{2} \alpha \gamma \frac{e^{\beta + \gamma \log(\omega_r)}}{(1 + e^{\beta + \gamma \log(\omega_r)})^2} \end{aligned} \quad (9)$$

Eq.(9) is analogous to Equation 2, where -

$$\xi_1 = -0.75729 - 0.04673 F_m - 0.000051 (C_u)^{2.4065} + 2.00944 \left( \frac{V_{beff}}{V_{beff} + V_a} \right) \quad (10)$$

$$\xi_2 = 0.43604 + 0.03399 (C_u)^{0.53471} - 0.74847 \left( \frac{V_{beff}}{V_{beff} + V_a} \right)^{0.30623} \quad (11)$$

$$\text{and, } \xi_3 = 3.53402 + 0.1047 F_m + 0.00064 (C_u)^{2.04946} - 6.12145 \left( \frac{V_{beff}}{V_{beff} + V_a} \right). \quad (12)$$

In Eq.(9), the values of  $\alpha$ ,  $\beta$ , and  $\gamma$  can be found from Eq.(5), Eq.(6), and Eq.(8), respectively.

## MODEL EVALUATION

The development of a regression-based model greatly depends on the statistical analysis and optimization process used. The fundamental aim of this type of model development process is to reduce the error from the prediction by comparing the predicted data with the observed data for the identical input variables. Optimization process involves the determination of regression coefficients in such a way that the developed equation provides minimum error when the predicted and observed data are compared. To determine the level of accuracy of the model, a statistical evaluation called “goodness of fit” is used. To determine “goodness of fit”, the estimated values by the developed models are compared with the tested or observed values at the same input conditions. Generally, two statistical parameters are required to be evaluated to

determine the “goodness of fit” of the model. The first one is the coefficient of determination ( $R^2$ ), and the second one is the ratio of the standard error ( $S_e$ ) to the standard deviation ( $S_y$ ). The mathematical form of  $R^2$ ,  $S_e$ , and  $S_y$  can be presented by the following expressions:

$$R^2 = 1 - \frac{(n-p-1)S_e^2}{(n-1)S_y^2}, \quad S_e = \left[ \frac{1}{(n-p-1)} \sum_1^n (\hat{x}_i - x_i)^2 \right]^{\frac{1}{2}}, \quad \text{and} \quad S_y = \left[ \frac{1}{(n-1)} \sum_1^n (x_i - \bar{x})^2 \right]^{\frac{1}{2}}. \quad (13)$$

In the above expressions,  $\hat{x}_i$  are the predicted data,  $x_i$  are the observed data,  $\bar{x}$  is the average of the observed data,  $n$  is the number of data points used in the model, and  $p$  is the number of fitting parameters used in the model. A relatively good predictive model would have a higher  $R^2$ , close to 1 and a smaller  $S_e/S_y$ .

**Dynamic Modulus Model.** The goodness of fit of the proposed  $|E^*(\omega)|$  model given in Eq.(4) was evaluated in two ways, i.e., in logarithmic scale and in normal or arithmetic scale. The developed  $|E^*(\omega)|$  model has a fairly good coefficient of determination ( $R^2 = 0.8373$ ) and a small  $S_e/S_y$  ( $S_e/S_y = 0.4047$ ) in normal or arithmetic scale. Again, in logarithmic scale these are:  $R^2 = 0.9027$ , and  $S_e/S_y = 0.3130$ , which are fairly good for this type of models where numerous complexities are involved. Figures 3(a) and 3(b) show the observed  $|E^*(\omega)|$  data versus the  $|E^*(\omega)|$  data predicted from the model in arithmetic and logarithmic scales, respectively. Both of the plots show that all the  $|E^*(\omega)|$  data points are around the line of equality (LOE) without any significant bias. Therefore, it can be said that the proposed dynamic modulus model based on  $|G_b^*(\omega)|$  gives a fairly good prediction of  $|E^*(\omega)|$  of the AC mixture typically used in New Mexico.

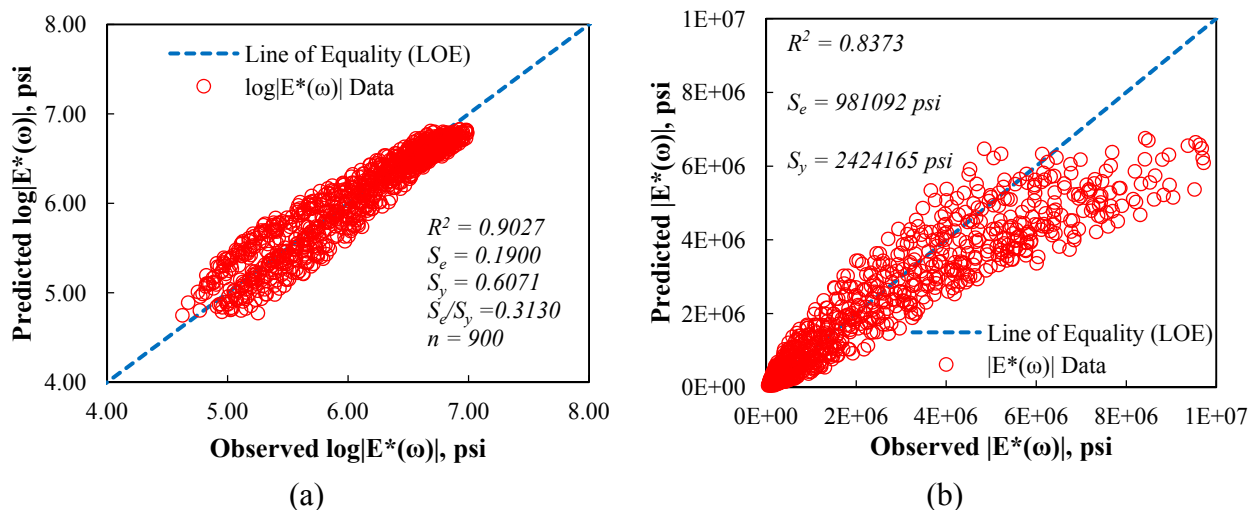


**Figure 3. Laboratory tested  $|E^*(\omega)|$  versus predicted  $|E^*(\omega)|$  plot in (a) logarithmic scale, and (b) arithmetic/normal scale.**

**Phase Angle Model.** In case of proposed  $\phi$  model, the goodness of fit is also evaluated. The developed  $\phi$ -model has a fairly good  $R^2 = 0.6967$  and a small  $S_e/S_y = 0.5526$ . Figures 4 shows the observed  $\phi$ -values versus the  $\phi$ -values predicted from the model given in Eq.(9). In this case, the plot shows that all the  $\phi$ -data points are around the line of equality (LOE) without any significant bias. Therefore, it can be said that the proposed phase angle model for asphalt concrete based on  $|G_b^*(\omega)|$  of the used binder gives a fairly good prediction of  $\phi$  of the AC mixture typically used in New Mexico.

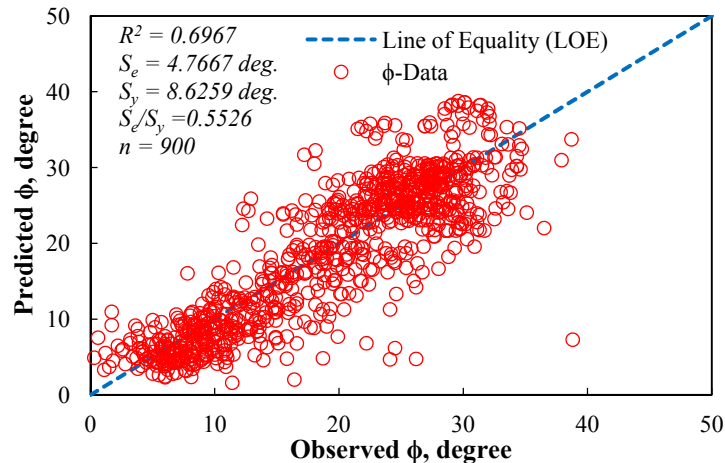


**Figure 4. Laboratory tested  $\phi(\omega)$  versus predicted  $\phi(\omega)$  for the AC samples.**

## CONCLUSIONS

In this study, new predictive models for dynamic modulus and phase angle of asphalt concrete are developed based on observed data of ten asphalt concrete mixtures typically used in New Mexico. The developed models use two fundamental aggregate gradation parameters: the fineness modulus and the uniformity coefficient, mix volumetric parameters (air void content and effective binder volume), and binder rheological parameters (dynamic shear modulus and binder phase angle) as direct input. The developed  $|E^*(\omega)|$  model possesses fairly good statistics, considering goodness of fit of the model.

## ACKNOWLEDGEMENTS

The authors would like to acknowledge the contributions of New Mexico Department of Transportation (NMDOT) for providing fund for this study.

## REFERENCES

- Andrei, D., Witzcak, M. W., and Mirza, M. W. (1999). *Development of a revised predictive model for the dynamic (complex) modulus of asphalt mixtures*. NCHRP 1-37, an Interim Rep., University of Maryland, College Park, Md.
- ASTM (1998). "ASTM D 2493 Viscosity-Temperature Chart for Asphalts," *Annual Book of ASTM Standards*, Vol. 0.403, 230-234.
- Bari, J. (2005). *Development of a new revised version of the Witzcak  $E^*$  predictive models for hot mix asphalt mixtures*, Ph.D. Dissertation, Arizona State University, Tempe, AZ.
- Bari, J., and Witzcak, M.W. (2006). "Development of a new revised version of the Witzcak  $E^*$  predictive model for hot mix asphalt mixtures (with discussion)," *J. of the Assoc. of Asphalt Pav. Tech.*, Vol. 75, 381–423.
- Birgisson, B., Sholar, G., and Roque, R. (2005). "Evaluation of a predicted dynamic modulus for Florida mixtures," *J. of the Transp. Res. Board*, Vol. 1929, 200–207.
- Ceylan, H., Gopalakrishnan, K., and Kim, S. (2008). "Advanced approaches to hot-mix asphalt dynamic modulus prediction," *Canadian J. Civil Eng.*, Vol. 35(7), 699–707.
- Ceylan, H., Schwartz, C. W., Kim, S., & Gopalakrishnan, K. (2009). "Accuracy of predictive models for dynamic modulus of hot-mix asphalt," *J. of Mat. Civil Eng.*, 21(6), 286–293.
- Christiansen, D. (2006). "Published discussion to 'Bari and Witzcak'," *J. of the Assoc. of Asphalt Pav. Tech.*, Vol. 75, 422–423.

- Christensen, Jr., D.W., Pellinen, T., and Bonaquist, R.F. (2003). "Hirsch model for estimating the modulus of asphalt concrete," *J. of the Assoc. of Asphalt Pav. Tech.*, Vol. 72, 97–121.
- Clyne, T.R., Li, X., Marasteanu, M.O., and Skok, E.L. (2003). *Dynamic and resilient modulus of Mn/DOT asphalt mixtures*, No. MN/RC-2003-09.
- Daniel, J. S., Kim, Y. R., and Lee, H. (2007). "Effects of Aging on Viscoelastic Properties of Asphalt-Aggregate Mixture," *J. Trans. Res. Board*, No. 1630, 21-27.
- El-Badawy, S., Bayomy, F., and Awed, A. (2012), "Performance of MEPDG dynamic modulus predictive models for asphalt concrete mixtures: local calibration for Idaho," *J. of Mat. Civil Eng.*, Vol. 24(11), 1412–1421.
- Hossain, Z., and Zaman, M. (2013). "Behavior of selected warm mix asphalt additive modified binders and prediction of dynamic modulus of the mixes," *J. of Testing and Evaluation*, Vol. 41, No. 1, 1-12.
- King, M., Momen, M., and Kim, Y.R. (2005). "Typical dynamic modulus values of hot-mix asphalt in North Carolina and their prediction," *84th Annual Trans. Res. Board Meeting*, Washington, D.C.
- Lee, K., Kim, H., Kim, N., and Kim, Y. (2007). "Dynamic modulus of asphalt mixtures for development of Korean pavement design guide," *J. Testing and Evaluation*, Vol. 35, No. 2, 1-8.
- Mohammad, L.N., Wu, Z., Myers, L., Cooper, S., and Abadie, C. (2005), "A practical look at simple performance tests: Louisiana's experience," *J. of the Assoc. of Asphalt Pav. Tech.*, Vol. 74, 557–600.
- Obulareddy, S. (2006). *Fundamental characterization of Louisiana HMA mixtures for the 2002 mechanistic-empirical design guide*. MS Thesis, Louisiana State University, LA.
- Rahman, A. S. M. A., Islam, M. R., and Tarefder, R. A. (2016). "Modifying the Viscosity Based Witczak Model and Developing Phase Angle Predictive Model for New Mexico's Superpave Mixes," *95th Annual Trans. Res. Board Meeting*, Paper No. 16-3180.
- Schwartz, C.W. (2005). "Evaluation of the Witczak dynamic modulus prediction model," *84th Annual Trans. Res. Board Meeting*, Paper No. 05-2112.
- Singh, D., Zaman, M., and Commuri, S. (2011). "Evaluation of predictive models for estimating dynamic modulus of hot-mix asphalt in Oklahoma," *J. of the Trans. Res. Board*, Vol. 2210, 57–72.
- Soleymani, H., Zhai, H., & Bahia, H. (2004). "Role of modified binders in rheology and damage resistance behavior of asphalt mixtures," *J. of the Trans. Res. Board*, Vol. 1875, 70–79.
- Tran, N.H., and Hall, K.D. (2005). "Evaluating the Predictive Equation in Determining Dynamic Moduli of Typical Asphalt Mixtures Used in Arkansas," *J. of the Assoc. of Asphalt Pav. Tech.*, Vol. 74, 1–17.
- Weldegiorgis, M. T., Faisal, H. M., and Tarefder, R. A. (2013). "Use of BBR Test Data to Enhance the Accuracy of  $|G^*|$ -Based Witczak Model Predictions," *Int. J. Pav. Conf.*, Paper No: 122-2, São Paulo, Brazil, 1-12.
- Weldegiorgis, M. (2014). *On dynamic modulus of asphalt concrete for moisture damage*, Doctoral Dissertation, Civil Engineering, University of New Mexico, Albuquerque, NM.